Innovative Systems Design and Engineering
ISSN 2222-1727 (Paper) ISSN 2222-2871 (Online)
Vol.6, No.2, 2015
www.iiste.org

Application of Permanent Magnets in Suspension and Recoil Buffer Systems

Dr. Tareq El-Hasan
Vice Dean Faculty of Engineering Technology, Zarqa University 132222, Zarqa 13132, Jordan

This research is funded by the Deanship of Scientific Research in Zarqa University /Jordan

Abstract

Rare Earth Permanent Magnets (PMs) has inspired new applications in areas where magnets were not used before due to their outstanding magnetic characteristics. PMs such as Neodymium Iron Boron and Samarium Cobalt are now used extensively in a wide range of applications such as electrical machines, transducers and loudspeakers, energy storage systems, hybrid and electric traction drives, etc. This paper is concerned with the application of modern permanent magnets in automotive suspension systems which may be potentially utilized for recoil buffer systems in defence applications in the future. The objective is to investigate the possibility of replacing the mechanical coil springs with strong PM rings in order to improve the suspension performance and ride comfort. The research is based on the existing suspension of a scooter model type Honda PCX 125. The as-is suspension is first analyzed and the system main parameters, such as dimensions, stiffness and damping coefficients are determined. Mathematical model for the proposed PM rings pull force is developed. Parametric analysis and optimization on the number of magnets and dimensions is performed to achieve the predetermined design requirements. A Matlab/Simscape model for the proposed PM spring model is developed and compared with the as-is rear suspension of the scooter. Results of the simulation are analyzed and conclusions and recommendations for further research are presented at the end of this paper.

Keywords: permanent magnet springs, suspensions system, Matlab/simscape model;

1. Introduction

Rare Earth Permanent Magnets (REPM) have become more important in today's technology and are increasingly used for a wide range of industrial applications. Neodymium Iron Boron (NdFeB) and Samarium Cobalt (SmCo) magnets are the strongest types of REPM commercially available [1] and [2]. They have replaced other types of PMs in many applications that require strong magnetic field, such as but not limited to:

- Electrical generators, motors and actuators
- Loudspeakers
- Sensors and transducers
- Hard disc drives
- Magnetic fasteners
- Magnetic levitations

NdFeB and SmCo magnets have magnetic characteristics that allow them to be used for such applications. The most important characteristics when considering a PM for a specific application are:

- High residual magnetic flux density, Br
- High coercive force (resistance to demagnetization), Hc
- High energy product, BH_{max} (high power density)

NdFeB and SmCo magnets are the heart of motors and generators that are used for aerospace industry due to their high power density. In addition, they are now being introduced into electric vehicles and wind power generation. As far as automotive industry is concerned, active and adaptive suspensions systems are attracting wide automobile manufacturers to improve passengers ride comfort. Many research activities have been focused on exploring the utilization of NdFeB and SmCo in such developing technologies [3] and [4]. Shock absorbers have been in the markets for long time and have been used extensively in several applications mainly in automotive, seismic and defense applications. Such traditional systems rely on the utilization of mechanical coil

springs as one of the main components required to withstand the loads applied to the systems.

Traditional suspension systems consisted of viscous shock absorbers, in parallel with suspension springs, have been widely used to reduce the vibration by dissipating the vibration energy into heat waste. To achieve better ride quality and road handling, active suspensions have been explored by many researchers [5]. However, it requires sophisticated system design and significant amount of energy, which limits its wide implementations. NdFeB magnets have strong magnetic capabilities which allow them to be used for magnetic levitation and suspensions systems. In this research, alternative suspensions design based on the utilization of NdFeB magnets have been proposed which has potential to improve suspension performance and quality of riding. The proposed design is implemented on a midsized scooter Honda PCX 125.

2. System Description

2.1 Scooter Description

For the purpose of the study of the proposed suspension in this research, the PCX 125 which stands as Honda's most advanced mid-sized scooter was selected. The PCX 125 with engine size of 125cc and 11.1 horse power is considered one of the most compact and economical motorcycles which was introduced in the market in late 2009. It is commonly characterized with its low-noise, low-emissions operation and ease of road handling. The PCX 125 scooter under consideration is depicted in Figure 1 and its main specifications are shown in Table I [6].

Table I: Honda PCX 125 Scooter main specifications

Specifications	Value
Engine size (cc)	125
Engine power (HP)	11.1
Curb weight (kg)	125
Dual front suspension with travel (mm)	100
Dual rear suspension with travel (mm)	74

2.2 Suspension System Description

The suspension of the scooter for each wheel consists of dual shock absorbers with dual coil springs as shown in Figure 2.

Figure 2. Dual rear and front suspensions of the SPX 125 scooter

For the purpose of simplification of the design and analysis in this research, half of the scooter with the rear suspension is considered. The suspension under consideration is shown in Figure 3 whereas the details of the coil spring of rear suspension are shown in Table II.

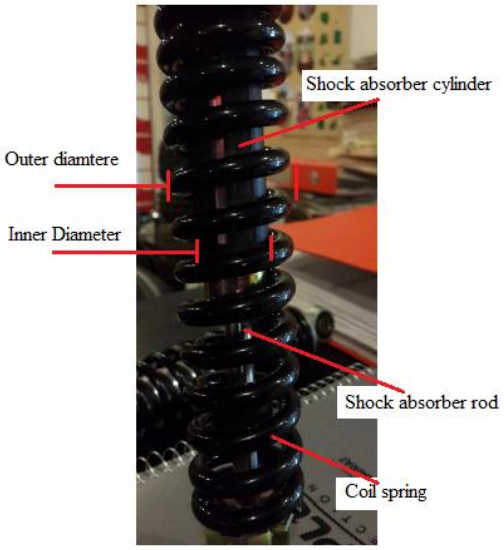

Table II: Details of the

Parameter	Value
Coil spring free length (mm)	255
Number of total coils	20
Number of active coils	18
Coil spring material	Phos-Brnz Grd A B159
Material shear modulus, G (GPa)	43.411
Coil Outer Diameter, OD (mm)	46
Coil Inner diameter, ID (mm)	34
Mean coil diameter, D (mm)	40
Wire diameter, d (mm)	6

Figure 3. Rear suspension shock absorber inside coil spring

The coils spring stiffness coefficient can be calculated as follows [7] and [8]:

$$K = \frac{Gd^4}{8nD^3} \qquad (1)$$

Where:

K is the coil spring stiffness coefficient in (N/m)

G is the spring material shear modulus in (Pa)

d is the wire diameter of the spring in (m)

D is the coil spring mean diameter in (m)

n is the number of active coils

The relationship between the applied force and coils spring stiffness coefficient can be expressed as:

$$F = K \cdot x \quad (2)$$

Where:

F is the vertical applied force on the spring in (N)

x is the spring vertical displacement in (mm)

For the shock absorber, the relationship between the applied force and the damping coefficient can be expressed as:

$$F = C \cdot v \quad (3)$$

Where v is the velocity of the damping in (m/s)

However, it was not possible to calculate the damping coefficient of the shock absorber theoretically. Therefore the shock absorber was sent to a local testing facility to determine its damping coefficient experimentally. The shock absorber measured damping coefficient and other coil spring calculated parameters using equations (1) and (2) are presented in Table III.

Table III: Rear suspension measured and calculated parameters

Parameter	**Value**
Measured shock absorber damping coefficient, *C* (N.s/m)	250
Calculated coil spring stiffness coefficient, *K* (N/m)	6105
Calculated coil maximum displacement, *x* (mm)	120
Calculated maximum allowable load, *F* (N)	730

3. Spring-Mass-Damper System modeling

Ignoring the tire effect, the whole system of the rear suspension of the scooter can be represented schematically by a simple series combination of spring, mass and shock absorber as shown in Figure 4.

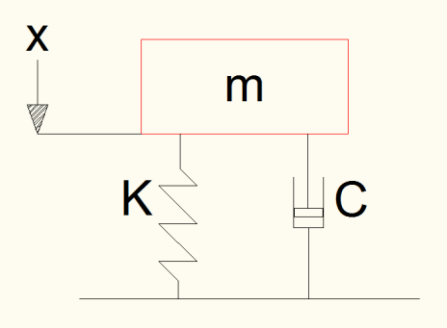

Figure 4. Graphical representation of one unit of the scooter rear suspension system

By giving the system shown schematically in Figure 4 an initial vertical displacement *Y*, it will vibrate freely with a time-varying function *y(t)*, and the resulting equation of motion will be [9] and [10]:

$$M\ddot{y} + C\dot{y} + Ky = 0 \quad (4)$$

To solve for *y(t)*; let $y(t) = Ve^{st}$ then the auxiliary equation and its solutions are:

$$Ms^2 + Cs + K = 0 \quad (5)$$

$$s = -\frac{C}{2M} \pm \sqrt{\frac{C^2}{4M^2} - \frac{K}{M}} \quad (6)$$

Substitute in *y(t)*, to get:

$$y(t) = Y_1 e^{S_1 t} + Y_2 e^{S_2 t} \tag{7}$$

$$y(t) = e^{-\frac{C}{M}t}\left[A_1 \sin\left(\sqrt{\frac{K}{M} - \frac{C^2}{4M^2}} \right) t + A_2 \cos\left(\sqrt{\frac{K}{M} - \frac{C^2}{4M^2}} \right) t \right] \tag{8}$$

But:

$$\xi = \frac{C}{C_{critical}} = \frac{C}{2\sqrt{KM}} \tag{9}$$

Where M is the mass of the rear part of the scooter ($M = 0.5m$) in (kg) and ξ is the damping ratio of the suspension system and may fall into one of the following ranges:

$\xi < 1$ or $C < C_{critical}$; under damped system

$\xi = 1$ or $C = C_{critical}$; critically damped system

$\xi > 1$ or $C > C_{critical}$: over damped system

The effect of damping ratio on the suspension system performance is depicted in Figure 5.

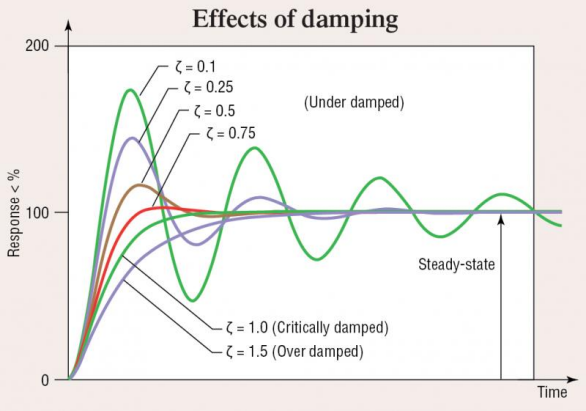

Figure 5. Typical effect of damping ratio on suspension system performance

To determine the critical frequency of the system, Equation (9) can be rearranged to get:

$$\omega_n = \sqrt{\frac{K}{M}} \tag{10}$$

and

$$f_n = \frac{\omega_n}{2\pi} \tag{11}$$

The performance characteristics for one unit of the rear suspension system can be determined based on Equations (9) and (10). The results obtained can be compared to the threshold values required to achieve comfort-ride criteria [11] as shown in Table IV.

Table IV: performance characteristics for one unit of the rear suspension system

Performance characteristics	**Calculated Value**	**"Ride comfort" value ***
Critical damping coefficient, $C_{critical}$ (N.s/m)	925	500 - 333
Damping ratio, ξ	0.27 (critically damped)	0.5 – 0.75
Natural frequency, f_n (Hz)	2.1	2.0 – 2.5
Peak deflection (mm) @ (75 x10) N impact	NA	50

* For sport car and motor cycles

4. Magnetic Spring Design

The proposed concept (Figure 6) is based on replacing the coil spring with specific number of ring magnets with certain thickness, inner diameter and outer diameter. To achieve the equivalent performance for the magnetic spring, the ring magnets of NdFeB are axially magnetized and carefully designed to achieve the required repulsive force.

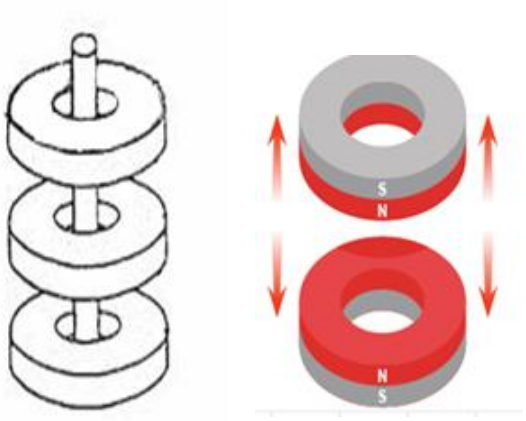

Figure 6. Proposed concept for the ring magnet spring

4.1 Magnetic Field Model

The magnetic fields created by the ring magnets have to be calculated in order to determine and optimize the required parameters of the magnetic spring. Most published analytical and numerical approaches have been focusing on determining the magnetic field along the center line of the ring magnets. Therefore a modified analytical model is required to calculate the magnetic field, hence the repulsive force along the gap between the two magnet surfaces. First, the magnetic flux density in the center of two opposite NdFeB ring magnets is developed based on the analytical models in [12], [13] and [14] as follows:

$$B_{g,\,center} = \frac{2*Br}{\pi} * \left[\tan^{-1}\left(\frac{\pi(R^2-r^2)}{2z\sqrt{4z^2+\pi^2(R+r)^2+(R-r)^2}} \right) - \tan^{-1}\left(\frac{\pi(R^2-r^2)}{2(t+z)\sqrt{4(t+z)^2+\pi^2(R+r)^2+(R-r)^2}} \right) \right]$$

Where:

$B_{g,center}$ is the flux density in the middle of the air gap between the ring magnet surfaces in (T)

Br is the residual flux density of the NdFeB ring magnets in (T)

R is the ring magnet outer radius in (m)

r is the ring magnet inner radius in (m)

t is the ring magnet axial thickness in (m)

Z is the axial half-distance between the ring magnets in (m)

The main parameters of equation (12) are defined on the ring model depicted in Figure 7.

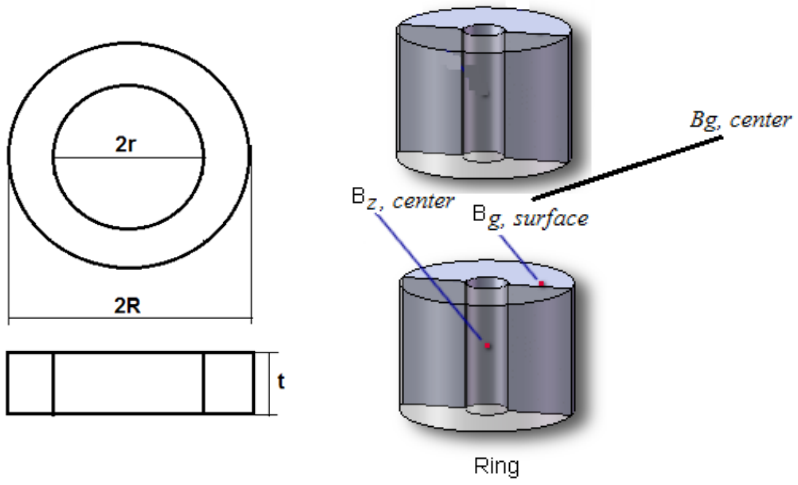

Figure 7. Main parameters defined for the ring magnets model

The repulsive magnetic force between two opposite ring magnets is determined as follows:

$$F = \frac{B_{g,center}^2 A}{2\mu_0} \qquad (13)$$

Where $A = \pi(R^2 - r^2)$ is the ring magnet surface area in (m^2) and $\mu_0 = 4\pi \times 10^{-7}$ is the air gap permeability in (H/m).

Substituting equation (12) in equation (13) the repulsive magnetic force between two opposite ring magnets is defined as:

$$F = \frac{4 * Br^2 (R^2 - r^2)}{\pi * \mu o} * \left[\tan^{-1}\left(\frac{\pi(R^2 - r^2)}{2z\sqrt{4z^2 + \pi^2 (R+r)^2 + (R-r)^2}} \right) - \tan^{-1}\left(\frac{\pi(R^2 - r^2)}{2(t+z)\sqrt{4(t+z)^2 + \pi^2 (R+r)^2 + (R-r)^2}} \right) \right]^2$$

For number of ring magnets (N), the total force is determined as:

$$F_T = \frac{4 * Br^2 (R^2 - r^2)(N-1)}{\pi * \mu o} * \left[\tan^{-1}\left(\frac{\pi(R^2 - r^2)}{2z\sqrt{4z^2 + \pi^2 (R+r)^2 + (R-r)^2}} \right) - \tan^{-1}\left(\frac{\pi(R^2 - r^2)}{2(t+z)\sqrt{4(t+z)^2 + \pi^2 (R+r)^2 + (R-r)^2}} \right) \right]^2$$

For a certain total axial length (L) of spring, and for a specific number of rings to occupy this length, the thickness of each ring magnet is calculated as follows:

$$t = \frac{[L - 2(N-1)Z]}{N} \qquad (16)$$

4.2 Parametric Analysis for Ring Magnet

Before performing the required calculations to determine the optimum design for the ring magnet spring, the main parameters that are used in the parametric analysis are defined as shown in Table V:

Table V: Parameters used for parametric analysis of the ring magnet spring

The process of parametric analysis summarized as follows:

Parameter	Value
Total Axial length, L (m)	Constrained @ 0.255
Axial distance between two ring magnets, 2Z (m)	Constrained @ 0.01
Number of ring magnets, N	Varied [2 – 16] in step of 1
Ring Magnet inner radius, r (m)	Constrained @ 0.0145
Ring Magnet outer radius, R (m)	Varied [0.02 – 0.03] in step of 0.001
NdFeB grades, Br (T)	1.22 @ N38 1.29 @N42

4.2.1 Define the NdFeB grade. This is necessary to set the value of the residual flux density *Br* of the ring magnets which is defined by the manufacturers of the NdFeB PM [15]. First, grade N38 is selected (Br = 1.22 T) and the necessary calculations are performed. Then grade N42 is selected (Br = 1.29 T) and the same calculations are repeated accordingly.

4.2.2 Vary the number of ring magnets (N). Once the magnet grade is set, the number of ring magnets is increased from 2 to 16 for each selected ring outer diameter (starting from R = 0.02 m), and the required ring magnet thickness is determined. The total force generated vs. number of ring magnet at different ring magnet outer radii is determined and the results obtained are graphically presented in Figure 8.

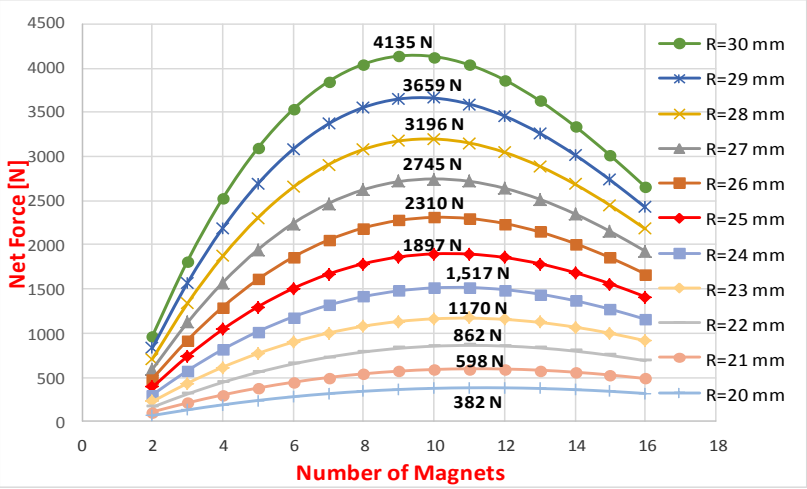

Figure 8. Ring magnet forces vs. number of magnets at different magnet outer radii

It is shown from Figure 8 that the optimum force is obtained at N = 11 magnets for R = 20 – 23 mm. The optimum force is shifted back to N = 10 magnets for R = 24 – 30 mm. It is also shown that increasing the ring magnet outer radius increases the total generated repulsive force. However, when considering the outer radius of the original coil spring as the geometrical limit for the design, it is found that at R = 23 mm, the total generated repulsive force (1170 N) is adequate enough to maintain the load/mass required for the proposed suspension design. Therefore all calculations will be performed on the ring outer radius R = 23 mm thereafter. Another graphical representation of the total repulsive force is described against the magnet axial thickness as shown in Figure 9.

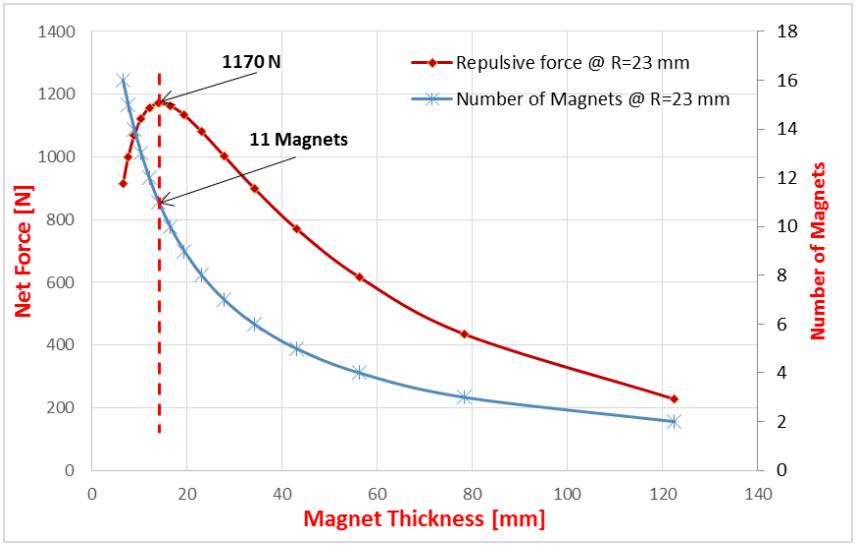

Figure 9. Total repulsive force and number of magnets vs. ring magnet thickness

4.2.3 Change the grade of magnet. At this stage, the ring magnet radius is set to *R*=23 mm and the magnet grade is changed from N38 to N42 thus changing *Br* from 1.22 T to 1.29 T respectively. The result for the total repulsive force vs. magnet thickness at the two different grades is graphically presented at Figure 10.

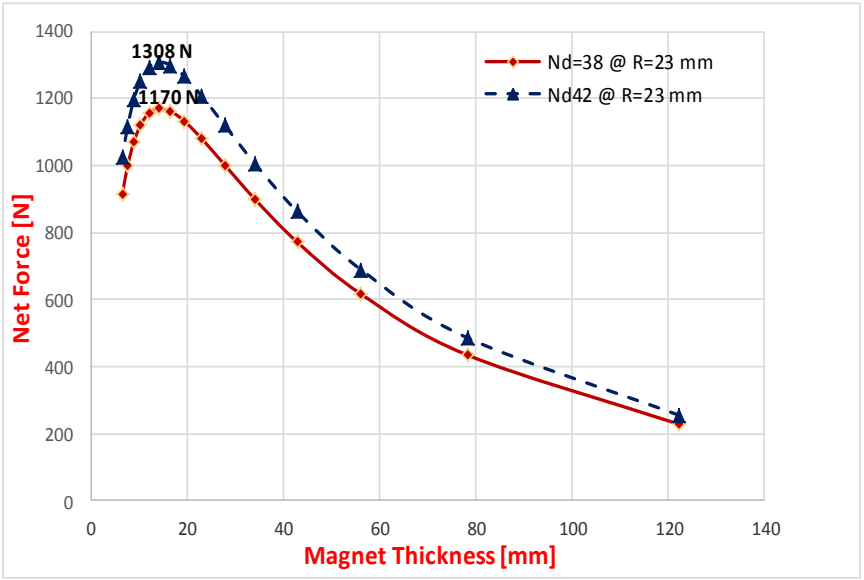

Figure 10. Total repulsive force vs. magnet thickness at different magnet grades

It is shown from Figure 10 that increasing the residual flux density by 5.73 % increases the total repulsive force by 11.8 %. The design parameters for the proposed magnetic spring as a result of the parametric analysis are summarized in Table VI.

Table VI: Design parameters for the proposed magnetic spring

Parameter	Value
Ring magnet axial thickness, t (m)	0.014
Number of ring magnets, N	11
Ring Magnet inner radius, r (m)	0.0145
Ring Magnet outer radius, R (m)	0.023
Mass of the total ring magnets, Mm (kg)	1.29
NdFeB grades	N38
Residual magnetic flux density, Br (T)	1.22

4.3 Determination of Magnetic Spring Stiffness.

To predict the stiffness coefficient for the proposed magnetic spring, the design parameters presented in Table VI are set for the calculation using Equation (15). In this case, the distance between the magnet Z is varied from 0 – 14 mm and the total repulsive force is calculated accordingly. Results for the behavior of the total repulse force vs. distance between ring magnets of grade N38 and N42 are depicted in Figure. 11.

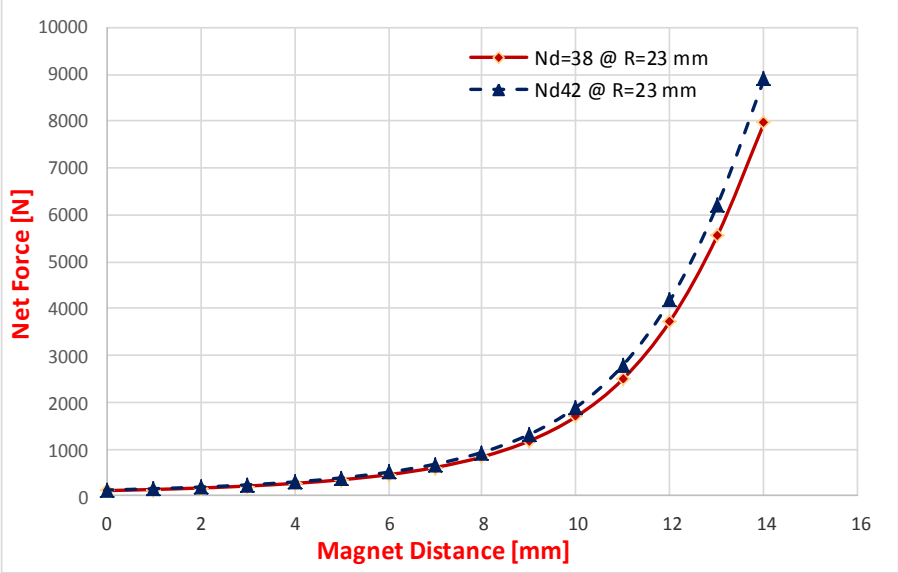

Figure 11. Total repulsive force vs. distance between ring magnets at different magnet grades

The results obtained from Figure 11 are useful to predict the stiffness coefficient of the proposed magnetic spring. In contrast to the mechanical coil spring, it is shown that the relationship between the force and the displacement is nonlinear. This means that the proposed magnetic spring has a variable stiffness rather than a constant stiffness coefficient. This in turn may have a positive impact on the performance of the suspension system and ride comfort of the scooter as will be discussed in the next sections.

4. Matlab/Simscape Model

In order to predict the performance of the proposed magnetic spring, a Matalb/simscape model was developed as depicted in Figure 12. The model simulates a drop test which represents a step force applied on both suspension models. The model considers the existing rear suspension system as well as the proposed magnetic spring by replacing the coil spring block with a custom developed block using simscape language [16] as shown in Appendix A. The custom block allows for nonlinear simulation of the proposed magnetic spring by entering the total repulsive forces and their corresponding displacements via a lookup table that is invoked when clicking on the custom block. The graphical user interface for the custom block is shown in Figure 13.

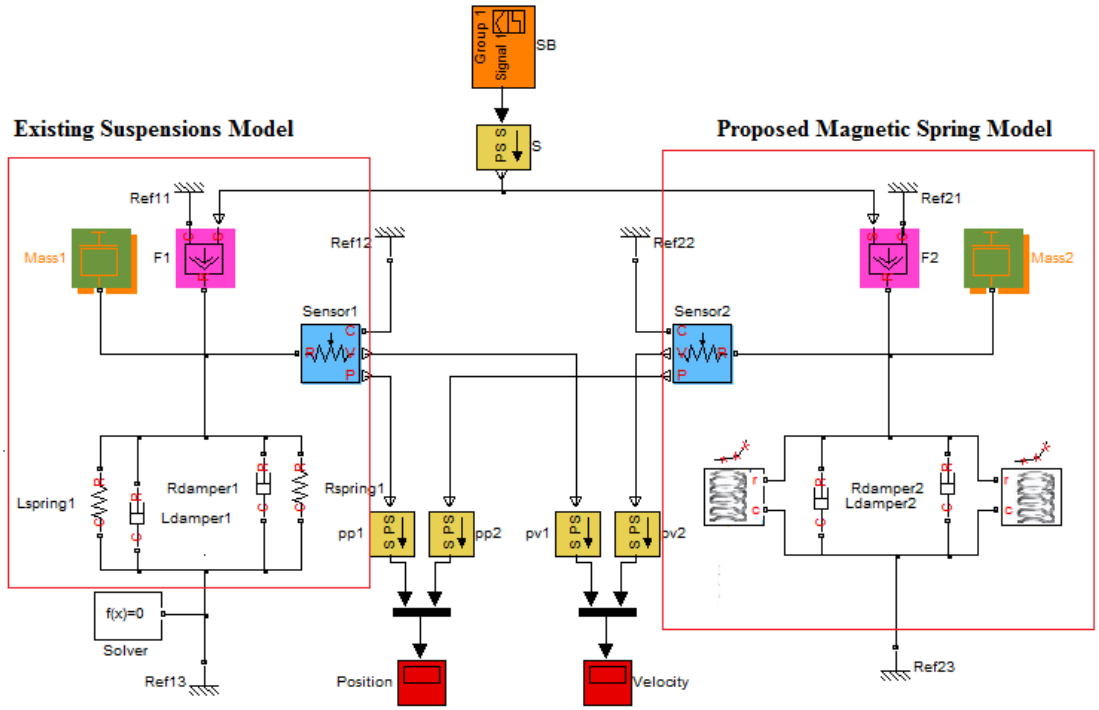

Figure 12. Matlab/simscape model for rear suspension (existing and proposed)

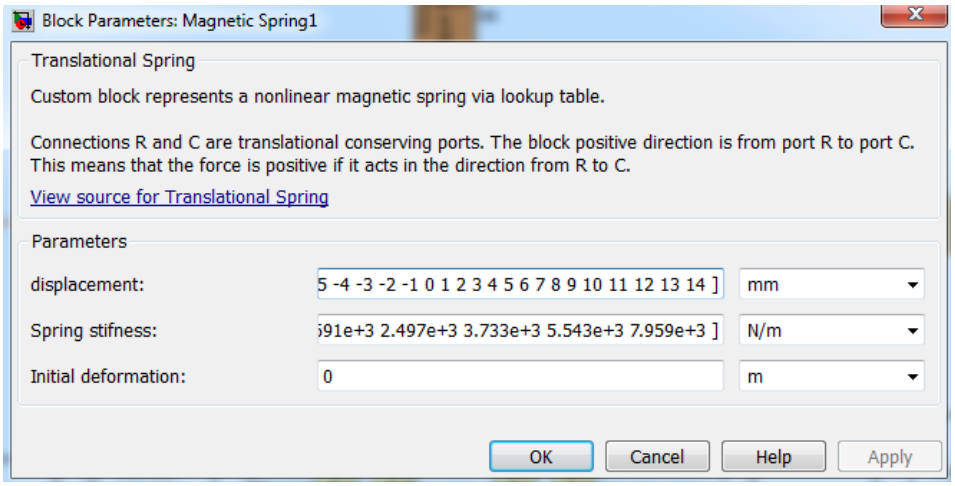

Figure 13. Custom block graphical user interface lookup table for the magnetic spring stiffness

To perform the simulation, the parameters of the existing (as-is) suspension which was presented in Table III are considered. The stiffness values of the proposed magnetic spring are extracted from the results which were obtained in Figure 11. The damping coefficient is kept the same for both models. The unsprung mass of the model is set to 75 kg to simulate half of the curb weight of the scooter. To simulate the drop test for both suspension models, each model is simultaneously subjected to a step force of 750 N using signal builder blocks. The outputs from the signal builder blocks are converted to physical signals using Simulink-PS converter blocks and fed to the ideal force source blocks. The applied force is then automatically applied to both suspension systems from which the displacement and velocity are picked via the translational motion sensor blocks. The results are then viewed by position scope and velocity scope as shown in Figure 14 and Figure 15 respectively.

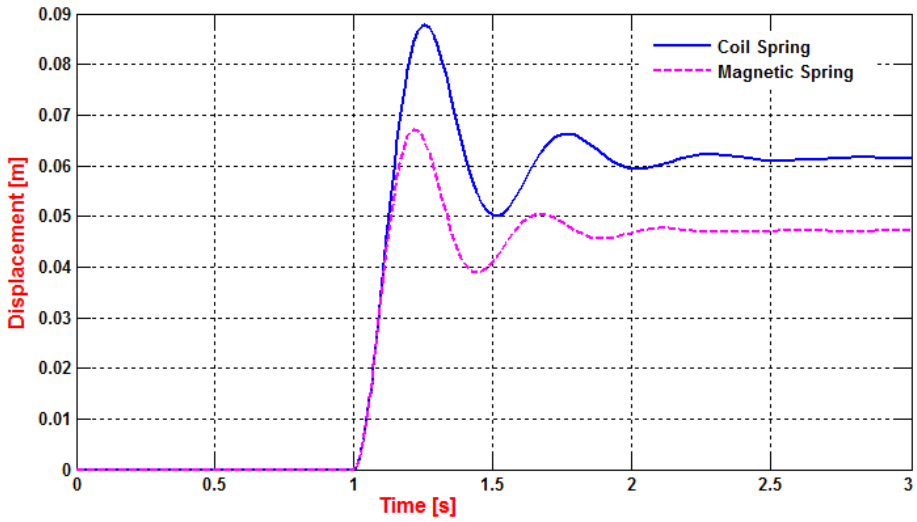

Figure 14. Simulation results for the displacement vs. time for both suspension systems

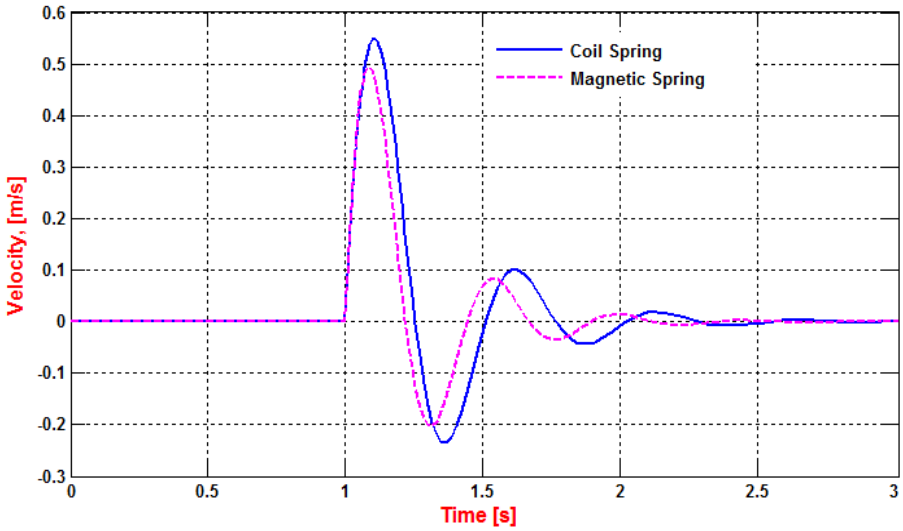

Figure 15. Simulation results for the velocity vs. time for both suspension systems

It is shown from Figures 14 that when using the proposed magnetic spring, the peak displacement is reduced by 23.8 % to an approximate value of 67 mm which is close to the ride comfort criteria (50 mm) as was presented in Table IV. It is also shown that a 47 mm final displacement is achieved using the magnetic spring compared to 62 mm displacement obtained from the coil spring. This results in improving the ground clearance for the scooter by approximately 24%. Figure 16 shows that a reduction of 11% in the velocity response is achieved when using the magnetic spring as compared to the coil spring model.

5. Conclusions and Recommendations for Future Work

In this research, a magnetic spring suspension using rare earth permanent magnet materials has been introduced as a replacement for the mechanical coil spring for the rear suspension of Honda PCX 125 scooter. The proposed magnetic spring which consists of set of axially magnetized rings magnets made from NdFeB were designed using parametric analysis. A total repulsive force of 1170 N was obtained through optimal design parameters from the set of 11 ring magnets. Results obtained demonstrated a nonlinear relationship between the repulsive force and the displacement of the spring. A half model for the scooter was simulated using Matlab/simscape where both coil spring and magnetic spring were compared in terms of ride comfort. Simulation results showed a

good potential for using the PM rings in automotive industry. The proposed magnetic spring has improved the ride comfort in two major aspects. Using magnetic spring, it was shown that the peak displacement was reduced by 24% whereas the peak response velocity was reduced by 11%. Moreover, the ground clearance of the scooter was under the maximum load was improved by 24%.

The results obtained from the analytical calculations and simulation unlocks the potential for utilizing the proposed magnetic spring for automotive application. Therefore a specific experimental test rig shall be developed to perform the drop test on both mechanical coil spring and the proposed magnetic spring. The objective is to validate the simulation results and to obtain characteristics performance that can be compared with the existing suspension model. The test can be performed as follows:

- The suspension shall be dynamically tested in the vertical position while installed in a suitable test fixture. A weight guided by a vertical rail shall be dropped from the required height necessary to emulate the operating energy input conditions.
- A temperature compensated electro-mechanical strain-gauged load pedestal shall be used to register shock force. A linear position transducer shall register the stroke of the unit. Force, and stroke data shall be plotted vs. time.
- Initially, an impacting mass shall be dropped from a specific height to achieve the required impacting speed. The drop weight and drop height maybe increased to obtain the proper energy input.

Once the proposed magnetic spring is tested and results are validated, modification on the system can be performed to control the stiffness of the spring electromagnetically. This may be achieved via several methods such as using coils wrapped around some magnetic cores around the magnet ring. By controlling the triggered coils and the amount of current in the triggered coils it is possible to achieve active or controlled suspension that are currently attracting numerous researches around the world [17] and [18]. Other potential application of the magnetic springs is their possible deployment in recoil buffer systems which may lead to a substantial reduction of the huge recoil forces exerted by massive weapons on vehicle's body.

6. Acknowledgment

The author extends his sincere gratitude to the Deanship of Scientific Research at Zarqa University /Jordan for funding and supporting this research.

References

S. Constantinides, "The Demand for Rare Earth Materials in Permanent Magnets, Arnold Magnetic Technologies 770 Linden Avenue.

Michael Weickhmann, "Nd-Fe-B Magnets, Properties and Applications" Vacuumschmelze GmbH & Co. KG, Hanau, Germany.

Jiajia Zheng, Zhaochun Li, JeongHoi Koo, Jiong Wang, "Magnetic Circuit Design and Multiphysics Analysis of a Novel MR Damper for Applications under High Velocity" Journal of Advances in Mechanical Engineering Volume (2014), Article ID 402501, http://dx.doi.org/10.1155/2014/402501

Kaja Mohideen, Msubash Ambed, Nithi Kumar, Udhaya Kumar, "Design and fabrication of magnetic shock absorber". http://www.academia.edu/3883802

M. D. Donahue J. K. Hedrick, "Implementation of an Active Suspension, Preview Controller for Improved Ride Comfort". The university of California at Berkeley 2001.

http://world.honda.com/PCX/spec/index.html

John C. Dixon, "The shock absorber handbook", 2nd edition, John Wiley & Sons 2007.

http://www.engineersedge.com/spring_comp_calc_k.html

Lei Zue, Pei-Sheng Zhang, "energy harvesting, ride comfort, and road handling of regenerative vehicle suspensions", ASME Journal of Vibration and Acoustics, 2012.

Unaune, M. J. Pawar, S. S. Mohite, "Ride Analysis of Quarter Vehicle Model", Proc. of the 1st International Conference on Modern Trends in Industrial Engineering, November 17-19, 2011.

Rober Q. Riely, "Automobile Ride, Handling, and Suspension Design With Implications for Low-Mass Vehicles", http://www.rqriley.com/suspensn.htm

J. M. Camacho, V. Sosa, "Alternative method to calculate the magnetic field of permanent magnets with azimuthal symmetry", Revista Mexicana de F´ısica E 59**,** JUNE 2013.

S. I. Babic, "Improvement In The Analytical Calculation Of The Magnetic Field Produced By Permanent Magnets" , Progress In Electromagnetics Research C, Vol. 5, pp. 71–82, 2008.

Ravaud,R.,G. Lemarquand,V. Lemarquand,and C. Depollier, "Analytical calculation of the magnetic field created by permanent-magnet rings," IEEE Trans. Magn.,Vol.44, No.8,pp. 1982–1989,Aug. 2008.

https://www.kjmagnetics.com/

Simscape language guide R2014b, www.mathworks.com

Shpetim Lajqi1, Stanislav Pehan, "Designs and Optimizations of Active and Semi-Active Non-linear Suspension Systems for a Terrain Vehicle", Journal of Mechanical Engineering 58(2012)12, 732-743.

Bart L. J. Gysen, Johannes J. H. Paulides, Jeroen L. G. Janssen, Elena A. Lomonova, Active Electromagnetic Suspension System for Improved Vehicle Dynamics", IEEE TRANSACTIONS ON VEHICULAR TECHNOLOGY, VOL. 59, NO. 3, pp. 1156 – 1163, MARCH 2010.

Appendix (A): Custom block for nonlinear magnetic spring

```
component magspring
% Translational Spring
% Custom block represents a nonlinear magnetic spring via lookup table.
% Connections R and C are translational conserving ports.
% The block positive direction is from port R to port C. This means that
% the force is positive if it acts in the direction from R to C.
nodes
    r = foundation.mechanical.translational.translational
    c = foundation.mechanical.translational.translational;
end
parameters (Size = variable)
xd = {[-14 -13 -12 -11 -10 -9 -8 -7 -6 -5 -4 -3 -2 -1 0 1 2 3 4 5 6 7 8 9
10 11 12 13 14],'mm' };  % displacement
kd = {[7959 5543 3733 2497 1691 1170 830 604 449 341 264 207 165 134 128
134 165 207 264 341 449 604 830 1170 1691 2497 3733 5543 7959],'N/m' }; %
Spring stiffness
x0 = {0,'m' } % Initial deformation
end
variables
    f = { 0,'N'};
    x = { 0,'m'};
    v = { 0,'m/s'}
    k = { 0,'N/m'}
end
function setup
    through (f, r.f, c.f);
    across (v, r.v, c.v);
    x = x0;
end
equations
      k == tablelookup(xd,kd,x,interpolation=linear,extrapolation=nearest);
      f == k * x
      v == x.der;
end
end
```

The IISTE is a pioneer in the Open-Access hosting service and academic event management. The aim of the firm is Accelerating Global Knowledge Sharing.

More information about the firm can be found on the homepage:
http://www.iiste.org

CALL FOR JOURNAL PAPERS

There are more than 30 peer-reviewed academic journals hosted under the hosting platform.

Prospective authors of journals can find the submission instruction on the following page: http://www.iiste.org/journals/ All the journals articles are available online to the readers all over the world without financial, legal, or technical barriers other than those inseparable from gaining access to the internet itself. Paper version of the journals is also available upon request of readers and authors.

MORE RESOURCES

Book publication information: http://www.iiste.org/book/

Academic conference: http://www.iiste.org/conference/upcoming-conferences-call-for-paper/

IISTE Knowledge Sharing Partners

EBSCO, Index Copernicus, Ulrich's Periodicals Directory, JournalTOCS, PKP Open Archives Harvester, Bielefeld Academic Search Engine, Elektronische Zeitschriftenbibliothek EZB, Open J-Gate, OCLC WorldCat, Universe Digtial Library , NewJour, Google Scholar